

Muscle hypertrophy driven by myostatin blockade does not require stem/precursor-cell activity

Helge Amthor^{a,b}, Anthony Otto^c, Adeline Vulin^a, Anne Rochat^a, Julie Dumonceaux^a, Luis Garcia^a, Etienne Mouisel^a, Christophe Hourd e^a, Raymond Macharia^d, Melanie Friedrichs^b, Frederic Relaix^a, Peter S. Zammit^e, Antonios Matsakas^c, Ketan Patel^f, and Terence Partridge^{f,1}

^aUniversit e Pierre et Marie Curie, Univ Paris 06, UMR S974 UMR S 787, Inserm, Institut de Myologie, AP-HP, Groupe Hospitalier de la Piti e-Salp tri re, F-75005, Paris, France; ^bDepartment of Pediatrics, University Hospital of Essen, 45147 Essen, Germany; ^cSchool of Biological Sciences, The University of Reading, Reading, RG6 6AJ, United Kingdom; ^dDepartment of Veterinary Basic Sciences, Royal Veterinary College, London, NW1 0TU, United Kingdom; ^eKing's College London, Randall Division of Cell and Molecular Biophysics, Guy's Campus, London, SE1 1UL, United Kingdom; and ^fCenter for Genetic Medicine Research, Children's National Medical Center, 111 Michigan Ave, NW, Washington, DC 20010

Edited by Eric N. Olson, University of Texas Southwestern Medical Center, Dallas, TX, and approved March 9, 2009 (received for review November 17, 2008)

Myostatin, a member of the TGF- β family, has been identified as a powerful inhibitor of muscle growth. Absence or blockade of myostatin induces massive skeletal muscle hypertrophy that is widely attributed to proliferation of the population of muscle fiber-associated satellite cells that have been identified as the principle source of new muscle tissue during growth and regeneration. Postnatal blockade of myostatin has been proposed as a basis for therapeutic strategies to combat muscle loss in genetic and acquired myopathies. But this approach, according to the accepted mechanism, would raise the threat of premature exhaustion of the pool of satellite cells and eventual failure of muscle regeneration. Here, we show that hypertrophy in the absence of myostatin involves little or no input from satellite cells. Hypertrophic fibers contain no more myonuclei or satellite cells and myostatin had no significant effect on satellite cell proliferation in vitro, while expression of myostatin receptors dropped to the limits of detectability in postnatal satellite cells. Moreover, hypertrophy of dystrophic muscle arising from myostatin blockade was achieved without any apparent enhancement of contribution of myonuclei from satellite cells. These findings contradict the accepted model of myostatin-based control of size of postnatal muscle and reorient fundamental investigations away from the mechanisms that control satellite cell proliferation and toward those that increase myonuclear domain, by modulating synthesis and turnover of structural muscle fiber proteins. It predicts too that any benefits of myostatin blockade in chronic myopathies are unlikely to impose any extra stress on the satellite cells.

muscle growth | muscular dystrophy | TGF-beta | muscle stem cells | myonuclear domain

Loss of muscle mass and strength is a major clinical feature of inherited myopathies such as Duchenne muscular dystrophy (DMD) and also of more common acquired atrophies associated with disuse, aging, and cancer. This loss has fostered widespread interest in the powerful inhibitory effect of myostatin, a member of the TGF- β family of signaling molecules, on muscle growth (1) with specific focus on the prospect of modulating this system to counteract atrophic processes. Indeed, muscle fiber hypertrophy arising from absence or blockade of myostatin has been reported to be associated with therapeutic benefits in the *mdx* mouse model of DMD (2, 3). This hypertrophy has been attributed to proliferation of satellite cells (4, 5), the principal cellular source for growing and regenerating skeletal muscle (6–10), consequent upon their release from myostatin inhibition (5, 11, 12).

Here, we have investigated the contribution of satellite cells in 2 myostatin-null mouse models, constitutive (*mstn*^{-/-}) and *compact* (*BEH*^{cl/c}), and following myostatin blockade by AAV-mediated overexpression of myostatin propeptide. These data, together with our results from in vitro studies on the effect of presence or absence of myostatin on satellite cells contradict comprehensively the widely held view that postnatal muscle

hypertrophy elicited by the blockade or absence of myostatin is the result of increased satellite cell activity.

Results

Lack of Myostatin Results Predominantly in Hypertrophy of Individual Muscle Fibers. Having shown previously that *mstn*^{-/-} extensor digitorum longus (EDL) muscles were 66% heavier than wild type (13), we analyzed their cellular composition. They contained only 11% more myofibers ($P = 0.026$) than controls but these myofibers were of 43% greater cross-sectional area ($P = 0.003$) and 6% longer ($P = 0.001$; Table 1; Fig. 1). Similarly, increased muscle size in the Berlin High mouse line *compact* (*BEH*^{cl/c}), which harbors a naturally occurring mutation in the *myostatin* gene (14, 15), reflects in part 37% more myofibers ($P = 0.023$) but, more importantly, a 93% larger mean fiber cross-sectional area ($P < 0.001$) and a significantly greater fiber length ($P < 0.001$) than *BEH*^{+/+} controls (supporting information (SI) Table S1). Thus, the large size of myostatin-deficient muscle is attributable chiefly to myofiber hypertrophy.

Muscle Fiber Hypertrophy Is Not Dependent on Satellite Cell Activity.

The number of myonuclei per myofiber reflects the cumulative history of muscle precursor recruitment during fiber growth. Surprisingly, EDL fibers of both *mstn*^{-/-} and *BEH*^{cl/c} mice contained fewer myonuclei per fiber ($P < 0.001$) than their respective wild-type controls (Table 1; Table S1; Fig. 1). This combination of larger size and fewer myonuclei must entail a markedly higher cytoplasmic-to-nuclear ratio.

Such a pattern of myostatin-null-induced hypertrophy suggests a lack of satellite cell recruitment. Immunostaining for Pax7, which is expressed as a marker of both quiescent and activated satellite cells (10), (Fig. 2A), we found fewer ($P < 0.001$) satellite cells per myofiber from *mstn*^{-/-} EDLs (3.2 ± 2.3 SD) than on equivalent wild-type myofibers (4.8 ± 3.0 SD) (Table 1; Figs. 1 and 2), with similar observations in *BEH*^{cl/c} ($P < 0.001$; Table S1). Thus, the sustained muscle hypertrophy arising from lack of myostatin is not associated with increase in either the number or recruitment of satellite cells. (Counts in 2 other muscles confirmed the lack of satellite cell increase in *mstn*^{-/-} mice: soleus,

Author contributions: H.A., A.O., J.D., L.G., F.R., K.P., and T.P. designed research; H.A., A.O., A.V., A.R., J.D., L.G., E.M., C.H., R.M., M.F., A.M., F.R., P.S.Z., and K.P. performed research; H.A., A.O., A.V., L.G., R.M., F.R., P.S.Z., K.P., and T.P. analyzed data; and H.A., K.P., and T.P. wrote the paper.

The authors declare no conflict of interest.

This article is a PNAS Direct Submission.

Freely available online through the PNAS open access option.

¹To whom correspondence should be addressed. E-mail: tpartridge@cnmcresearch.org.

This article contains supporting information online at www.pnas.org/cgi/content/full/0811129106/DCSupplemental.

Table 1. Cellular morphometric properties of male *Mstn*^{-/-} and C57BL/6 wild-type EDL muscles

Variable	Age (months)	<i>Mstn</i> ^{-/-}	C57BL/6 wild type	<i>P</i> *
Number of myofibers	7	1,200 ± 71 (5)	1,083 ± 65 (5)	0.026*
Fiber area (μm ²)	7	3,192 ± 507 (5 mice, 974 fibers)	2,235 ± 293 (6 mice, 1,251 fibers)	0.003*
Satellite cells per fiber	2	3.2 ± 2.3 (212 fibers, 4 mice)	4.8 ± 3.0 (272 fibers, 6 mice)	<0.001*,**
Myonuclei per fiber	2	244.5 ± 52 (212 fibers, 4 mice)	261.3 ± 53 (244 fibers, 5 mice)	<0.001*,**
Fiber length (μm)	2	4,047 ± 529 (89 fibers, 3 mice)	3,820 ± 457 (117 fibers, 4 mice)	0.001*

Values are given as means together with standard deviation; number of muscles examined is given in parentheses. *, for statistical analysis unpaired *t*-test and **, Kolmogorov-Smirnov 2-sample test were used and *P* below 0.05 considered as significant.

wild type, 9.6 ± 3.5, *n* = 84; *mstn*^{-/-}, 10.4 ± 4.0, *n* = 90; biceps brachii, wild type, 3.9 ± 2.1, *n* = 64; *mstn*^{-/-}, 3.1 ± 1.9, *n* = 65.)

Satellite Cell Proliferation Is Independent of Myostatin. To examine the direct effect of myostatin on myoblast proliferation we monitored the rate of increase in satellite cell numbers around isolated myofibers in tissue culture growth medium. This constitutes a biologically relevant model of the basic self-replacing muscle unit, standardizing myoblast proliferation to the variability both in number and behavior of fiber-associated satellite cells (16, 17), (Fig. 2*B*). After 72 h in culture, fewer myoblasts

(43 ± 32 SD) had accumulated in cultures from 2-month-old *mstn*^{-/-} mice than in those from age-matched wild-type mice (58 ± 35 SD; *P* < 0.001; Fig. 3*A*). Although starting numbers of cells per fiber were smaller in the former, the gradients, indicating rates of increase in cell number, are indistinguishable. Moreover, blockade of any potential contaminant myostatin in the serum and chicken embryo extract with J16-mouse anti-myostatin monoclonal antibody did not affect the number of

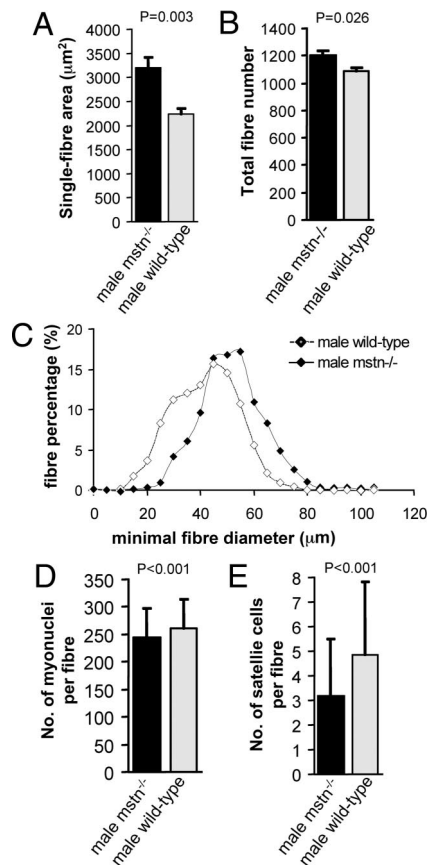


Fig. 1. Morphometric and cellular properties of EDL muscles from adult male *mstn*^{-/-} mice compared to age-matched C57BL/6 wild types. (A) Total fiber number of whole EDL muscles from *mstn*^{-/-} mice (black column) compared to wild types (gray column) (*P* = 0.026). (B) EDL fiber area from *Mstn*^{-/-} mice (black column) compared to wild types (gray column) (*P* = 0.003). (C) Fiber size distribution in the EDL from *mstn*^{-/-} mice (black diamonds) and wild-type mice (white diamonds). (D) Number of myonuclei per isolated muscle fiber from EDL muscles from *mstn*^{-/-} mice (black column) compared to wild types (gray column) (*P* < 0.001). (E) Number of Pax-7 positive satellite cells per isolated muscle fiber from EDL muscles from *mstn*^{-/-} mice (black column) compared to wild types (gray column) (*P* < 0.001).

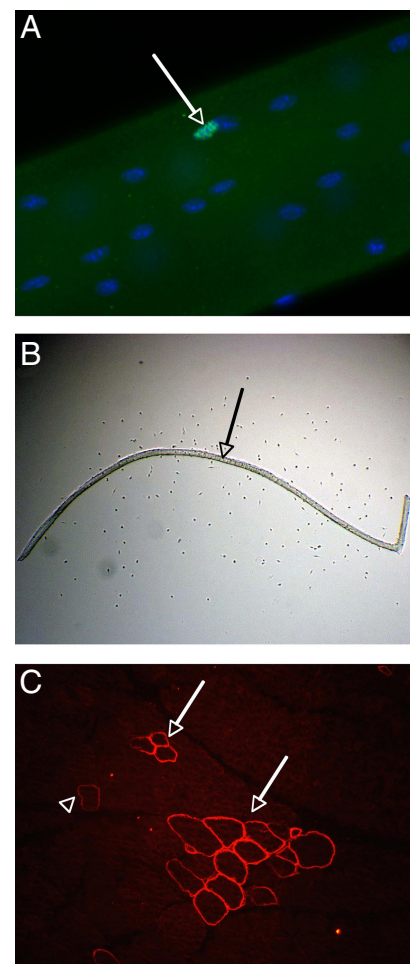


Fig. 2. Analysis of muscle fibers. (A) Part of an isolated fiber from wild-type EDL, combined immunostaining against Pax-7 (green), and nuclear stain with DAPI (blue). The image depicts 1 satellite cell (arrow) and numerous myonuclei. (B) Example of a culture of an isolated muscle fiber (arrow) from wild-type EDL muscle after 3 days of in vitro incubation. Numerous myoblasts are present in the proximity of the muscle fiber, which are visible as little dots at this magnification in phase microscopy. (C) Immunostaining against revertant fibers on a cross-section of EDL muscle from *mstn*^{+/+/mdx} mouse depicts 2 clusters of revertant fibers (3 and 13 revertant fibers, respectively, arrows) and 1 paler isolated revertant fiber (arrowhead).

Table 2. Morphometric properties after injection of AAV myostatin propeptide into tibialis anterior muscles compared to AAV-MSeap injection

Variable	Days postinjection	AAV-prop	AAV-MSeap	<i>P</i> *
Muscle weight (mg)	14*	44.72 ± 2.92 (6)	38.76 ± 2.38 (6)	0.038
	28*	50.10 ± 2.77 (6)	39.05 ± 0.55 (6)	0.0003
	42*	51.55 ± 2.40 (6)	40.12 ± 1.49 (6)	0.00033
	56*	49.98 ± 4.32 (6)	39.05 ± 0.97 (6)	0.002
	70*	48.63 ± 2.3 (6)	41.20 ± 1.23 (6)	0.0021
Number of myofibers	28*	3,245.8 ± 59.5 (5)	3,184.6 ± 71.5 (5)	0.729
	56*	3,328 ± 131 (5)	3,420 ± 72 (5)	0.47
Fiber area (μm ²)	28*	2,242 ± 163 (16,035 fibers, 5 mice)	1,996 ± 91 (16,238 fibers, 5 mice)	0.089
	56*	2,156 ± 41 (16,763 fibers, 5 mice)	1,865 ± 116 (16,200 fibers, 5 mice)	0.004
Myonuclei per fiber	31**	0.65 ± 0.06 (475 fibers, 4 mice)	0.63 ± 0.07 (816 fibers, 4 mice)	0.774
Myonuclei/surface area (<i>n</i> ^{E-05} /pixel)	31**	3.4 ± 0.48 (4 mice)	4.5 ± 0.38 (4 mice)	0.031
Myf5 + ve cells/100 fibers	31*	3.2 ± 2.5 (6 mice)	2.4 ± 0.8 (6 mice)	0.31

AAV injections were performed into TA muscles of C57Bl6 mice at 8 weeks of age* or at 6 weeks of age**. Values are given as means together with standard deviation; number of muscles examined is given in parentheses; for statistical analysis paired *t*-test was used and *P* < 0.05 considered as significant.

(*P* = 0.25; Table S2), again showing no effect of lack of *myostatin* on *mdx* muscle regeneration.

As a further indicator of regenerative activity, we analyzed the frequency of dystrophin-positive “revertant” fibers found sporadically in both *mdx* and DMD muscles (Fig. 2C). Progressive expansion of revertant fiber clusters has been shown to be a cumulative indicator of satellite cell-dependent muscle regeneration (27). Comparison of revertant fiber frequency in EDL muscles from *mstn*^{-/-}*mdx* mice and *mstn*^{+/+}*mdx* mice revealed no significant difference in total numbers, in numbers per cluster, or the numbers of isolated revertant fibers (Table S2; Fig. S2); further argument against any significant boost of net regenerative activity of dystrophic muscle in the absence of myostatin.

Discussion

Together, the above data comprehensively challenge the generally accepted mechanism of action of myostatin on satellite cells in postnatal muscle. On the contrary, it attributes postnatal muscle hypertrophy generated by lack of myostatin largely to hypertrophy of individual fibers that owes little or nothing to satellite cell activity, being generated mainly by increase in size of the myonuclear domain. True, the larger number of fibers in the genetically myostatin-null mice, especially in the *BEH*^{fl/c} strain, does imply some excess proliferation of muscle progenitors during early muscle development. This accords with our detection of expression of activin receptors at prenatal stages and aligns with recent demonstrations that, during early myogenesis, myostatin acts to limit myogenic cell proliferation by favoring their entry into terminal differentiation (28). Even then, the larger-than-normal size of muscle fibers in the myostatin-null adults involved no increase in numbers of myonuclei per fiber, implying some limiting influence other than myostatin on the numbers of myogenic cells fusing into individual fibers over their period of formation and growth. Moreover, blockade of myostatin in postnatal muscle produced no evidence for either de novo generation of muscle fibers or for any increase in myonuclei per myofiber profile. Furthermore, in the dystrophic *mstn*^{-/-}*mdx* mice, enhanced muscle growth was not attributable to an increase above normal levels of muscle regeneration. This lack of responsiveness of postnatal satellite cells to myostatin signaling is explicable by their perinatal downregulation of activin receptors.

Our *in vitro* data supporting this view are in agreement with previous studies employing similar concentrations of myostatin (29) but conflict with a previous publication employing 10- to 20-fold higher concentrations (4). The essentially artifactual

nature of tissue culture leaves open the debate as to what the biologically appropriate doses and individual tissue culture conditions are for evaluation of myostatin activity. However our *in vivo* findings firmly contradict the notion that myostatin-mediated control of satellite cell proliferation has any significant influence on muscle fiber hypertrophy during normal postnatal growth or during regeneration of dystrophic muscle. This revelation points us away from the signaling pathways of satellite cell activation and proliferation that are linked to the accepted view of myostatin action (11), in both normal postnatal and regenerating myopathic muscle. It implicates, instead, mechanisms whereby myostatin regulates protein balance within the muscle fibers themselves. This accords well with recent biochemical studies of muscle hypertrophy in myostatin null conditions (30, 31), finding little or no concordant increase in DNA content and thus attributing much of the effect to enlargement of the myonuclear domain, with associated increased transcription of myofibrillar RNAs. A recent debate concluded that the relationship between muscle fiber hypertrophy and myonuclear number was variable between models and situations (32). Our data places the fiber hypertrophy associated with lack of myostatin activity at the extreme in which large size of muscle fibers mainly reflects enlargement of myonuclear domain. It implies, too, that this mechanism, rather than augmented satellite cell activation, operates even in regenerating dystrophic muscle in which satellite cells are actively proliferating in response to the stimuli that mediate muscle repair.

From a practical viewpoint, we need to revise current views that therapeutic strategies based on myostatin blockade counteract muscle defects by stimulating satellite cell activity. Such an adjustment does not conflict with a recent report on the effect of myostatin blockade in adult muscular dystrophy patients, which showed a tendency toward bigger muscle fibers with no evidence of increased muscle regeneration (33). But the change in rationale would usefully inform the design of future human clinical trials of myostatin blockade such as those in DMD. The implication that beneficial amounts of muscle hypertrophy are independent of satellite cell activity raises the prospect of combating forms of muscle weakness such as disuse atrophy that are not directly associated with satellite cell function. It is important, however, before further clinical trials, to explore the consequences of an increased myonuclear domain on homeostasis and physiological function of muscle tissue: specifically its relationship to the severe decrease in specific force and the mitochondrial depletion observed in myostatin-deficient muscle (13).

Methods

Animals. *Mstn*^{-/-} founder breeding pairs on a C57BL/6 background were a gift of Se-Jin Lee (Johns Hopkins University, Baltimore) (1). Myostatin knockout

and wild-type mice (C57BL/6) were bred and kept in the animal facilities of The Royal Veterinary College, London, under guidelines of the Home Office (UK) under license PPL/70/5218.

Muscles from a subline of the Berlin High mouse line (BEH), which is homozygous for the compact mutation (13–15, 34), were a kind gift from Lutz Bunker. Muscles from 1.5-year-old male *mstn*^{-/-}*mdx* mice and *mstn*^{+/-}*mdx* littermates were a kind gift from Kathryn Wagner (Johns Hopkins University, Baltimore) (3). *Myf5*^{nlaZ/+} mice (20) and *Pax3*^{GFP/+} mice (21) were bred in the animal facilities of the UMR-S 787, Medical Faculty Pitié-Salpêtrière, under institutional guidelines.

Production and Injection of AAV Vector. The myostatin propeptide construct was prepared by PCR amplification of C57BL6 cDNA and introduced into an AAV-2-based vector under the control of the CMV promoter. The AAV-muSeAP was described elsewhere (35). (Production details appear in supporting information.)

Single Fiber Isolation and Culture. EDL muscles were carefully dissected from mice killed by cervical dislocation. Age and number of animals are given in Tables 1 and 2; Tables S1 and S2. Myofibers isolated as described previously (36, 37) were either fixed in 4% PFA/PBS or cultured as detailed in *SI Text* (36, 37).

Immunohistochemistry of Single Muscle Fibers. Fixed myofibers were permeabilized with 0.5% (vol/vol) Triton X-100/PBS and blocked with 20% (vol/vol) goat serum/PBS, as described previously (36). Satellite cells were visualized with anti-Pax-7 antibody (DSHB) and Alexa Fluor 488 goat anti-mouse IgG (Molecular Probes) before mounting in Faramount fluorescent mounting medium (DakoCytomation) containing 100 ng/mL DAPI.

Morphometric Analysis of *mstn*^{-/-} and Compact Mice. EDL muscles were weighed and then mounted in OCT (BDH) and frozen in melting isopentane cooled in liquid nitrogen. Ten-micrometer transverse sections from the mid-belly were cut on a cryostat and total number was counted in H&E-stained transverse sections using Leica QWin software. Minimal and maximal fiber diameters and fiber area of all fibers were determined using KS 300 software (Carl Zeiss). Number and age of mice are given in Table 1 and [Table S1](#).

Histological Analysis of AAV-Injected Muscles. After killing of AAV-injected mice, both tibialis anterior muscles were removed, weighed, mounted in OCT, and frozen in isopentane cooled in liquid nitrogen. Transverse cryostat sections (8 μ m) were fixed in 2% paraformaldehyde for 30 min, blocked for 1 hour in 1% BSA, 1% sheep serum, 0.1% triton X-100, and 0.001% sodium azide before incubation with a rabbit anti-laminin antibody (Dako, Z0097, 1/300) followed by Cy3-conjugated goat anti-rabbit IgG secondary antibody (Jackson

ImmunoResearch, 111–165-144, 1/200). After immunostaining for laminin, fiber number, and CSA, and myonuclear number and position were analyzed by Ellix software (Microvision).

LacZ-expressing nuclei were visualized in *Myf5*^{nlaZ/+} mice and counted, together with myonuclei, on 2 complete transverse cryostat sections (10 μ m) of each AAV-injected TA muscle using standard protocols for X-Gal staining. Most X-Gal positive nuclei were found adjacent to the sarcolemma and designated satellite cells; the occasional X-Gal positive nucleus found within muscle fibers, was not included in the satellite cell counts.

Real-Time Quantitative PCR. Real-Time PCR was performed according to standard protocols on a DNA Engine Opticon 2 System (Bio-Rad) as detailed in supporting information.

FACS Sorting of Pax3 Positive Cells. Isolation and cell sorting of GFP+ cells were performed as previously described (24). Expression of the receptors was normalized to *MyoD* expression to make conservative allowance for the lower frequency of activation of postnatal satellite cells.

Statistical Analysis. All values are expressed as mean \pm standard deviation. To determine significance between 2 groups, we made comparisons using the unpaired Student's *t*-tests and Kolmogorov-Smirnov 2-sample test for comparison of different mouse genotypes and paired Student's *t*-tests for comparison of ipsilateral and contralateral muscles. *P* < 0.05 was considered statistically significant.

ACKNOWLEDGMENTS. We thank Elaine Shervill, Helen Hunt, and Daniela Kittel for excellent technical assistance. We are indebted to Professor Se-Jin Lee for providing founder mice for our *mstn*^{-/-} colony, Professor Kathryn Wagner for providing *mstn*^{-/-}*mdx* muscles, and Dr. Lisa-Anne Whittemore and Dr. Simon Hughes for providing antibodies. The work was funded by The Wellcome Trust (066195 and 078649 to R.M. and K.P.) and the Biotechnology and Biological Sciences Research Council (11020 to K.P. and A.O.). H.A. is supported by the Muscular Dystrophy Association (3870), the Bundesministerium für Bildung und Forschung (as member of the *MD-NET*, 01 GM0302, Project R24), and by the Association Monégasque contre les Myopathies. C.H.'s postdoctoral salary is supported by the Association Monégasque contre les Myopathies. F.R. is supported by the Inserm Avenir program, AFM strategic plan to UMR-S 787 and Decryphon program. A.R.'s postdoctoral salary is supported by the Decryphon program to F.R. The laboratory of P.S.Z. is supported by The Medical Research Council, The Muscular Dystrophy Campaign, the Association of International Cancer Research, and the Association Française contre les Myopathies. T.A.P. is supported by funding from the Wellstone Center (U54HD053177), and the United States Department of Defense Congressionally Directed Medical Research Program (W81XWH-05-1-0616).

- McPherron AC, Lawler AM, Lee S-J (1997) Regulation of skeletal muscle mass in mice by a new TGF- β superfamily member. *Nature* 387:83–90.
- Bogdanovich S, et al. (2002) Functional improvement of dystrophic muscle by myostatin blockade. *Nature* 420:418–421.
- Wagner KR, McPherron AC, Winik N, Lee SJ (2002) Loss of myostatin attenuates severity of muscular dystrophy in mdx mice. *Ann Neurol* 52:832–836.
- McCroskery S, Thomas M, Maxwell L, Sharma M, Kambadur R (2003) Myostatin negatively regulates satellite cell activation and self-renewal. *J Cell Biol* 162:1135–1147.
- McCroskery S, et al. (2005) Improved muscle healing through enhanced regeneration and reduced fibrosis in myostatin-null mice. *J Cell Sci* 118:3531–3541.
- Moss FP, Leblond CP (1971) Satellite cells as the source of nuclei in muscles of growing rats. *Anat Rec* 170:421–435.
- Mauro A (1961) Satellite cell of skeletal muscle fibers. *J Biophys Biochem* 9:493–495.
- Collins CA, et al. (2005) Stem cell function, self-renewal, and behavioral heterogeneity of cells from the adult muscle satellite cell niche. *Cell* 122:289–301.
- Sherwood RI, et al. (2004) Isolation of adult mouse myogenic progenitors: Functional heterogeneity of cells within and engrafting skeletal muscle. *Cell* 119:543–554.
- Zammit PS, et al. (2004) Muscle satellite cells adopt divergent fates: A mechanism for self-renewal? *J Cell Biol* 166:347–357.
- McFarlane C, et al. (2008) Myostatin signals through Pax7 to regulate satellite cell self-renewal. *Exp Cell Res* 314:317–329.
- Wagner KR (2005) Muscle regeneration through myostatin inhibition. *Curr Opin Rheumatol* 17:720–724.
- Amthor H, et al. (2007) Lack of myostatin results in excessive muscle growth but impaired force generation. *Proc Natl Acad Sci USA* 104:1835–1840.
- Szabo G, et al. (1998) A deletion in the myostatin gene causes the compact (Cmpt) hypermuscular mutation in mice. *Mamm Genome* 9:671–672.
- Varga L, et al. (1997) Inheritance and mapping of Compact (Cmpt), a new mutation causing hypermuscularity in mice. *Genetics* 147:755–764.
- Bockhold K, Rosenblatt J, Partridge T (1998) Aging normal and dystrophic mouse muscle: Analysis of myogenicity in cultures of living single fibers. *Muscle Nerve* 21:173–183.
- Heslop L, Morgan JE, Partridge TA (2000) Evidence for a myogenic stem cell that is exhausted in dystrophic muscle. *J Cell Sci* 113:2299–2308.
- Hill JJ, et al. (2002) The myostatin propeptide and the follistatin-related gene are inhibitory binding proteins of myostatin in normal serum. *J Biol Chem* 277:40735–40741.
- Lee SJ, McPherron AC (2001) Regulation of myostatin activity and muscle growth. *Proc Natl Acad Sci USA* 98:9306–9311.
- Tajbakhsh S, et al. (1996) Gene targeting the *myf-5* locus with *nlaZ* reveals expression of this myogenic factor in mature skeletal muscle fibers and early embryonic muscle. *Dev Dyn* 206:291–300.
- Relaix F, Rocancourt D, Mansouri A, Buckingham M (2005) A Pax3/Pax7-dependent population of skeletal muscle progenitor cells. *Nature* 435:948–953.
- Qiao C, et al. (2008) Myostatin propeptide gene delivery by adeno-associated virus serotype 8 vectors enhances muscle growth and ameliorates dystrophic phenotypes in mdx mice. *Hum Gene Ther* 19:241–254.
- Relaix F, et al. (2006) Pax3 and Pax7 have distinct and overlapping functions in adult muscle progenitor cells. *J Cell Biol* 172:91–102.
- Montarras D, et al. (2005) Direct isolation of satellite cells for skeletal muscle regeneration. *Science* 309:2064–2067.
- Bulfield G, Siller WG, Wight PA, Moore KJ (1984) X chromosome-linked muscular dystrophy (mdx) in the mouse. *Proc Natl Acad Sci USA* 81:1189–1192.
- Sicinski P, et al. (1989) The molecular basis of muscular dystrophy in the mdx mouse: A point mutation. *Science* 244:1578–1580.
- Yokota T, et al. (2006) Expansion of revertant fibers in dystrophic mdx muscles reflects activity of muscle precursor cells and serves as an index of muscle regeneration. *J Cell Sci* 119:2679–2687.
- Manceau M, et al. (2008) Myostatin promotes the terminal differentiation of embryonic muscle progenitors. *Genes Dev* 22:668–681.

29. Wagner KR, Liu X, Chang X, Allen RE (2005) Muscle regeneration in the prolonged absence of myostatin. *Proc Natl Acad Sci USA* 102:2519–2524.
30. Welle S, Bhatt K, Pinkert CA (2006) Myofibrillar protein synthesis in myostatin-deficient mice. *Am J Physiol Endocrinol Metab* 290:E409–415.
31. Welle S, Bhatt K, Pinkert CA, Tawil R, Thornton CA (2007) Muscle growth after postdevelopmental myostatin gene knockout. *Am J Physiol Endocrinol Metab* 292:E985–991.
32. O'Connor RS, Pavlath GK, McCarthy JJ, Esser K (2007) A last word on point:counterpoint: Satellite cell addition is/is not obligatory for skeletal muscle hypertrophy. *J Appl Physiol* 103:1107.
33. Wagner KR, et al. (2008) A phase I/II trial of MYO-029 in adult subjects with muscular dystrophy. *Ann Neurol* 63:561–571.
34. Bunger L, et al. (2001) Inbred lines of mice derived from long-term growth selected lines: Unique resources for mapping growth genes. *Mamm Genome* 12:678–686.
35. Bartoli M, et al. (2007) AAV-mediated delivery of a mutated myostatin propeptide ameliorates calpain 3 but not alpha-sarcoglycan deficiency. *Gene Ther* 14:733–740.
36. Beauchamp JR, et al. (2000) Expression of CD34 and Myf5 defines the majority of quiescent adult skeletal muscle satellite cells. *J Cell Biol* 151:1221–1234.
37. Rosenblatt JD, Lunt AI, Parry DJ, Partridge TA (1995) Culturing satellite cells from living single muscle fiber explants. *In Vitro Cell Dev Biol Anim* 31:773–779.